

Nanoscale

Accepted Manuscript



This is an *Accepted Manuscript*, which has been through the Royal Society of Chemistry peer review process and has been accepted for publication.

Accepted Manuscripts are published online shortly after acceptance, before technical editing, formatting and proof reading. Using this free service, authors can make their results available to the community, in citable form, before we publish the edited article. We will replace this *Accepted Manuscript* with the edited and formatted *Advance Article* as soon as it is available.

You can find more information about *Accepted Manuscripts* in the [Information for Authors](#).

Please note that technical editing may introduce minor changes to the text and/or graphics, which may alter content. The journal's standard [Terms & Conditions](#) and the [Ethical guidelines](#) still apply. In no event shall the Royal Society of Chemistry be held responsible for any errors or omissions in this *Accepted Manuscript* or any consequences arising from the use of any information it contains.

Light Induced Aggregation of Specific Single Walled Carbon Nanotubes

Madhusudana Gopannagari¹ and Harsh Chaturvedi^{1†}

¹Department of Physics, Indian Institute of Science Education and Research, Pune-411008, INDIA

ABSTRACT: We report optically induced aggregation and consequent separation of specific diameters of nanotubes from stable solution of pristine single walled carbon nanotubes (SWNTs). Dispersed solutions of pristine SWNTs in different solvents show rapid and selective aggregation. Separated SWNTs show enrichment in specific diameter of SWNTs aggregating out under UV, visible and NIR illumination.

KEYWORDS: Light, aggregation, Separation, Single Walled Carbon Nanotubes.

[†] Corresponding Author E-mail: hchaturv@iiserpune.ac.in

Single walled carbon nanotube (SWNT) -based materials have applications in electro-optics, plasmonics, and biotechnology.¹⁻³ Moreover, dispersion of nanoparticles like one dimensional SWNTs, also provides with an opportunity to understand the effects of electro-optical forces on intermolecular interactions.⁴ SWNTs are commonly dispersed in solution and functionalized with other molecules and polymers for fabrication of devices and sensors.⁵⁻⁷ Dispersion of SWNTs produces a mixture of various diameters of metallic and semiconducting SWNTs.⁸ Separation of specific SWNTs from solution is an important concern and various methods are being employed including density gradient, gel-chromatography and using surfactants, polymers and other functional molecules.⁹⁻¹³ Photophoretic forces are predicted to play an important role for chiral and diameter specific separation of SWNTs from solution.¹⁴ We recently reported photophoresis in aggregates of SWNTs in solution.¹⁵ Although optically induced aggregation especially in nanoparticles has theoretically been predicted and reasonably reported, very few experimental proofs of aggregation of nanoparticles by light could be found.^{16, 17} Optical induced aggregation in gold nanoparticles¹⁸ and specifically in SWNTs functionalized with optically active supra-molecules has been reported.^{19, 20} Stability of a solution depends on the dimensions, uniform surface charges and dielectric properties of the interacting particles and solution.⁴ Under significant optical excitation, photophoretic forces in resonating particles are expected to affect the colloidal stability, leading to subsequent aggregation of the absorbing SWNTs. Here, we report optically induced aggregation of selective pristine SWNTs from dispersed solution. Well-dispersed, stable solution of pure, pristine SWNTs in solution show enhanced rate of aggregation under optical illumination by simple UV, broadband visible and NIR light. Optically induced rate of aggregation depends on the frequency and on the intensity of applied illumination. Significantly, the aggregated floc of SWNTs shows enrichment in selective diameter of

nanotubes, specific to the frequency of the applied illumination. Hence, we report, the phenomenon of optically induced aggregation and its potential application in efficient separation of different diameter of nanotubes from solution. Such optical methods may play an important role for efficient large scale, non-intrusive, separation of specific diameters from pure SWNTs, without any functionalization or creation of defects due to chemical processes.

Well dispersed, stable solutions of pristine SWNTs were prepared by ultrasonication of 0.6 mg of SWNT (Nano Integris®-IsoNanotubes, 95% purity) in 100 mL of N,N-Dimethylformamide (DMF) (Sigma Aldrich®). Pristine SWNTs have diameter distribution from ~ 0.7nm to 1.7 nm, and average length expected to be 300 nm to 1.7nm. Solutions were found stable for weeks. Care was taken to avoid water absorption and light exposure. Stable solutions of dispersed pristine SWNT were exposed to UV light (125 W, 352 nm), broadband visible light (125 Watts) and NIR light (Fuzi, 150Watts) between 30-240 mins. Control samples were kept in the dark for the same time and used to calculate the normalized rate of aggregation for SWNTs in presence of light. Samples kept in light and dark were centrifuged @ 8000 rpm (Eppendorf® Mini Spin Centrifuge Machine) for 10 min to carefully separate the supernatant from the solution. Separated supernatant and flocs were analyzed by UV-Vis-NIR spectrophotometer (Perkin Elmer® Lambda 950 UV-Vis spectrometer) and Raman spectrometer (632 nm Laser).

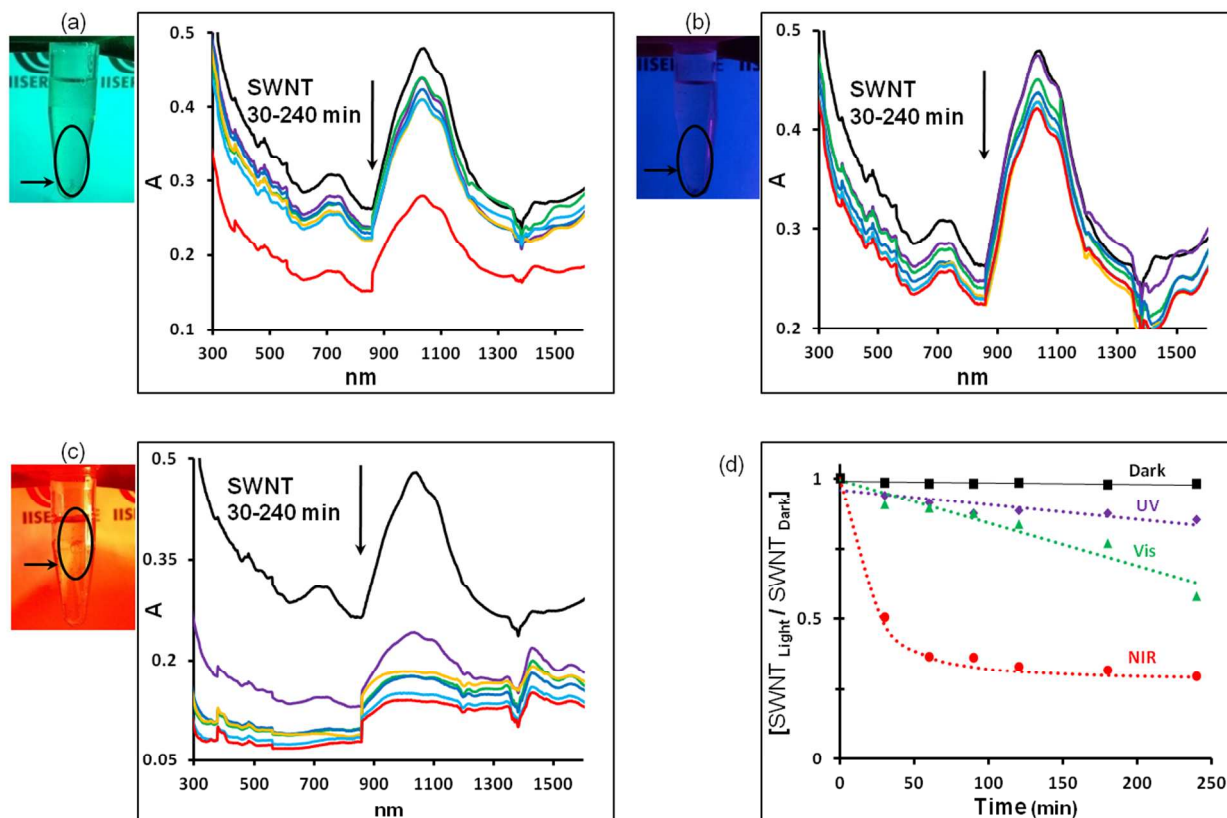


Figure 1. Light induced aggregation in broadband visible (a), UV (b) and NIR lamps (c) are shown. After 240 mins illumination of time aggregated floes are shown in an arrow. Absorption spectra of supernatant collected from pure SWNTs under UV, visible and NIR lamps show consistent decrease in concentration when exposed to varying duration from 30 mins to 240 mins (d) shows relative rate of optically induced aggregation in Pristine SWNTs under UV, visible and NIR illumination.

The absorption spectra of pure SWNTs show cumulative absorption by different diameters of nanotubes in solution. As shown in **Figure 1**, the absorption spectra of pure SWNTs shows background plasmonic resonance in UV (300-450 nm) due to metallic SWNTs and van Hove singularities due to band-gap absorption in the visible and NIR by semiconducting SWNTs. Absorption by the pristine SWNTs in the NIR frequency (850-1400 nm) is attributed to the S_{11}

band-gap absorption by semiconducting SWNTs of specific diameters.²¹ Individual absorption peak intensities, representing electronic transitions in the NIR S_{11} band of semiconducting SWNTs are sensitive to relative concentration of SWNTs with specific tube diameters and chirality. Along with a consistent decrease in the concentration of the separated supernatant of pristine SWNTs by varying the time of optical exposure, indicating optically induced aggregation, **Figure 1(a-c)** also shows discernible changes in both the UV and in the visible-NIR frequency of the supernatant suggesting selective aggregation of different diameter of SWNTs. Supernatants separated from the solution exposed to NIR illumination for different times (**Figure 1c**), distinctly shows consistent changes and enrichment with specific diameter of SWNTs. Optically induced aggregation was observed for pristine SWNTs exposed to broadband visible, UV and NIR illumination. Rate of optically induced aggregation was determined using absorption spectroscopy as shown in **Figure 1(a-c)**. Concentration for each supernatant was normalized with reference to the stable concentration of the sample kept in dark. Concentration at 840nm was used to determine the rate of aggregation as the spectra here is relatively flat and free of van Hove singularities. Rate of aggregation was plotted with respect to time of exposure for each sample under different lamps. At the maximum exposure time of 240 minutes, about 20% and 40% of SWNT aggregates out under UV and broadband visible illumination respectively, however rapid aggregation was observed under NIR illumination with 65% SWNTs aggregating, as shown in **Figure 1(d)**.

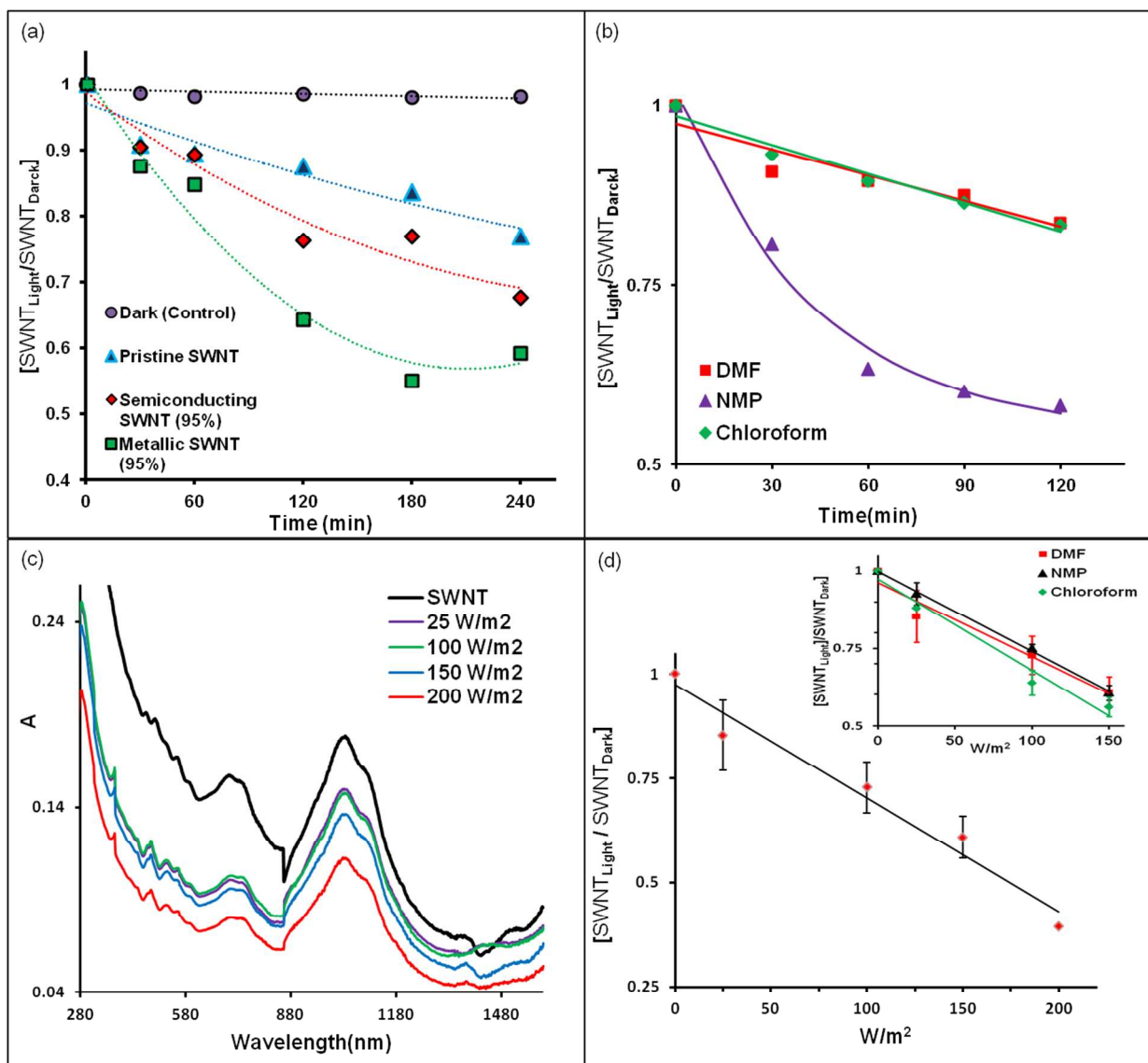


Figure 2. (a) Light induced rate aggregation in Pristine (un-separated), Semiconducting (95% Pure) and Metallic (95% Pure) SWNTs in DMF, under broadband visible illumination. (b) Optically enhanced, rate of aggregation in different solvents. (c) Absorption spectra of the supernatant, separated from the pristine SWNTs after exposure to visible illumination for varying intensities. (d) SWNTs dispersed in DMF showing rapid increase in the rate of aggregation with increase in the visible intensity. Inset: SWNTs dispersed in NMP and Chloroform showing similar rate of optically induced aggregation as in DMF.

This phenomenon of optically induced aggregation of pristine SWNTs in DMF was further studied using pre separated 95% pure metallic and semiconducting SWNTs. Pre separated SWNTs were brought from Nanointegris and were dispersed in DMF without any further modifications. Along with the dispersion of SWNTs in DMF; stable solution of pristine SWNTs in NMP, Chloroform were also prepared, by the similar method of ultra-sonication as reported above. Rapid aggregation of SWNTs were observed in each of the SWNT solutions under broadband (UV-Vis) illumination. Metallic SWNTs show higher rate of aggregation than semiconducting or pristine SWNTs as shown in **Figure 2 (a)**.

Un-separated pure SWNTs dispersed in different organic solvents (DMF, NMP, Chloroform) were exposed to broadband halogen lamp for varying time intervals (30-240 min). Samples were then centrifuged and supernatant separated from the aggregated SWNTs. Similar to the optically induced aggregation observed in DMF, supernatant separated from the SWNTs dispersed in NMP and Chloroform also, show consistent decrease in the concentration of SWNTs with corresponding increase in the exposure time. Concentration of the SWNTs in the supernatant was normalized with the stable pristine SWNT solution, kept in dark (control). Corresponding graph plotted in **Figure 2(b)** shows similar optically induced rate of aggregation for NMP and DMF, however rate of aggregation is found to be 20% more rapid in case of SWNTs dispersed in Chloroform. Experiments show that optically induced aggregation in SWNTs depends on the type of the SWNTs (Metallic and Semiconducting) and the solvent used.

This phenomenon of optically induced aggregation was further studied by varying the intensity of the visible lamp. Solution of SWNTs dispersed in each of the organic solvents (DMF, NMP and Chloroform) was exposed to visible lamp for 1 hour with varying intensities (25-150 W/m²). **Figure 2(c)** shows absorption spectra of the supernatant separated from the optically aggregated

SWNTs in DMF solution. As shown in **Figure 2(d)**, the concentration of SWNTs dispersed in all three organic solvents (DMF, NMP and Chloroform) show linearly enhanced rate of aggregation, with corresponding increase in the intensity of visible illumination. Interestingly when exposed for varying time intervals, SWNTs dispersed in chloroform show much rapid aggregation as compared to SWNTs dispersed in NMP and DMF; However, for different intensities of same visible illumination, SWNTs in all the three solvents show similar rate of aggregation.

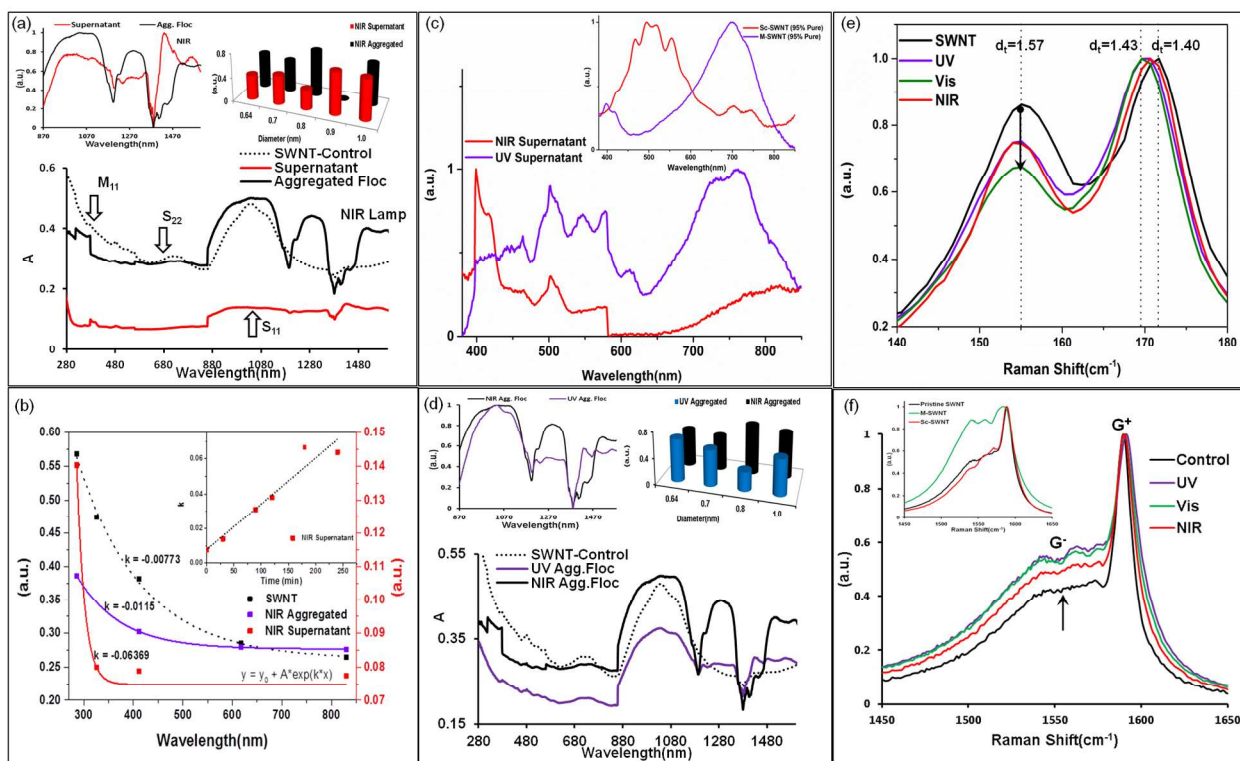


Figure 3. (a) Absorption spectra of the supernatant and aggregated floc as separated from the pristine SWNT (dotted line) after 240 mins exposure to NIR illumination and normalized NIR bands (Left Inset). Histogram showing enrichment of specific diameters in the separated supernatant and aggregated SWNTs (b) shows increase in the Extinction coefficient (k) of SWNTs in the supernatant with increase in the time of exposure from NIR illumination. (c) Normalized absorption spectra of the supernatants separated from the pristine SWNT solution after UV and NIR illumination. Inset shows absorption spectra for reference solution of pre

separated, pure metallic and semiconducting SWNTs. (d) Absorption spectra of aggregated floc under UV and NIR light illumination and normalized NIR bands (Left Inset). Histogram of showing enrichment in specific diameters (e) Shows RBM (d) G band Raman spectra of optically aggregated SWNTs, exposed to UV, visible and NIR illumination.

Diameter (d_t) of the semiconducting SWNTs may be calculated using the absorption in the NIR frequency (λ_{11}) by $\lambda_{11} = \frac{hcd_t}{2a_{c-c}\gamma_0}$. Where, c-c bond distance is measured to be 0.142 nm, and $\gamma_0=2.7$ eV is the interaction energy.²² **Figure 3(a)** show substantial differences in the absorption spectra of the supernatant and aggregated floc, separated from the solution of pristine SWNTs, after exposing to NIR illumination for 240 mins. Significant changes in the normalized NIR band (850-1500 nm) of the separated supernatant and floc are shown in **Figure 3(a)** [left Inset]. Variations in the NIR peak intensity and frequency is associated with the changes in the relative distribution of the different diameters of the semiconducting SWNTs in the solution. Histogram in **Figure 3(a)** [Right inset] shows relative enrichment in different diameters of semiconducting SWNTs in the separated supernatant and optically, aggregated floc. This distribution of different diameters of semiconducting SWNTs in a solution is calculated by fitting multiple lorentzian peaks to the normalized absorption in the NIR frequency (900-1400 nm). While the diameter of SWNT is estimated by the frequency of the peak, intensity of the normalized peaks depends on the relative enrichment of SWNT of that specific diameter.

Exponential increase in the background absorption of pristine SWNTs in UV-visible range of (300-500nm) is attributed to plasmonic resonance due to metallic SWNTs. Extinction coefficient for each of the absorption spectra in **Figure 1 (c)** was calculated by fitting exponential fits in the 300-500 nm frequency range. **Figure 3(b)** shows different exponential fits to the absorption spectra of the supernatant and aggregated floc, separated from the pristine SWNTs

after NIR illumination for 240 mins. Inset **Figure 3(b)** shows consistent increase in the extinction coefficient of the separated supernatant with increase in the time of exposure to NIR illumination. This consistent increase in the extinction coefficient of the separated supernatant indicates corresponding decrease in the plasmonic resonance due to metallic SWNTs. Absorption spectra of the supernatant separated after NIR exposure from 30 mins -240 mins (**Figure 1(a)**) show consistent loss of background resonance indicating aggregation of metallic SWNTs and increase in specific diameters of semiconducting SWNTs in the separated supernatant. Exponential background absorption due to plasmonic resonance by metallic SWNTs was subtracted from the absorption spectra of the supernatants separated after exposure to NIR and UV illumination for 240 mins. With background plasmonic absorption subtracted, **Figure 3(c)** shows sharp van hove singularities due to band gap absorption by semiconducting SWNTs of different diameters. Significant discernible changes are observed in the absorption peaks of supernatants of pristine SWNTs separated after UV and NIR illumination. Inset **Figure 3(c)** shows absorption peaks from the reference solution of metallic (95% pure) and semiconducting SWNTs (95% pure). Supernatant separated after exposure to NIR illumination show significant enrichment in specific diameters of SWNTs absorbing at 400 nm; whereas, supernatant separated from UV exposure shows significant enrichment in SWNTs absorbing around 750nm. Comparing the absorption spectra of optically separated supernatants with the reference solution of pure metallic and semiconducting SWNTs, it is inferred that supernatant separated after NIR illumination shows enrichment in selective diameters of semiconducting SWNTs whereas, supernatant separated after UV exposure shows enrichment in specific diameter of metallic SWNTs.

Similar to **Figure 3(a)**, **Figure 3(d)** compares the diameter distribution in the SWNTs aggregating under UV and NIR illumination. Discernible changes are also observed in the Radial Breathing Mode RBM mode (**Figure 3e**) and G band (**Figure 3f**) Raman spectra of the optically aggregated flocs separated from the pristine SWNT after exposure to UV, visible and NIR illumination.

RBM mode of pristine SWNTs depends on the diameter of the nanotube.²³ RBM of the aggregated SWNTs under different illuminations shows distinct enrichment of specific diameter of SWNTs which can be calculated using the relation $\omega_{RBM} = (\alpha_{RBM}/d) + \alpha_{bundle}$.²¹ Where, α_{RBM} , α_{bundle} are constants associated with bundling effect and scaling factor in RBM spectra of nanotubes respectively and d is the diameter of the SWNT corresponding to the RBM peak frequency (ω_{RBM}). As calculated from the expression, RBM of aggregates shows relative enrichment in following diameters 1.42, 1.43, 1.41 nm when exposed to UV, Visible or NIR illumination respectively. Consequent changes are also seen in SWNTs with larger diameters of 1.57 nm corresponding to the RBM frequency of $\sim 155 \text{ cm}^{-1}$. Changes in the G band Raman spectra of pristine SWNTs indicates significant changes in the relative concentration of metallic and semiconducting SWNTs.^{24, 25} **Figure 3 (f)**, shows considerable changes in the normalized G band, indicating increase in metallic SWNTs aggregating under UV, visible and NIR illumination as compared pristine SWNT solution. G-band Raman spectra of the reference, pre separated metallic and semiconducting SWNTs are shown in **Figure 3(f)** inset. The inset shows considerable increase in G band for metallic SWNTs (95%) as compared to semiconducting SWNTs (95%). Hence, the RBM and G band Raman spectra do indicate enrichment in aggregating SWNTs of specific diameters and changes in the ratio of metallic and semiconducting SWNTs depending on the frequency of optical illumination.

This phenomenon of optically induced aggregation in selective SWNTs may be due to photophoretic and photo-thermal processes in SWNTs.²⁶ Induced photophoretic motion by similar lamps in aggregates of metallic and semiconducting SWNTs have recently been reported.¹⁵ Similar photophoretic forces, along with photo-thermal processes may be responsible for selective aggregation of pristine SWNTs. Even with inherent limitations due to various assumptions of surface charges, geometry and dielectrics, aggregation of SWNT dispersions are still widely explained using conventional DLVO theory.²⁸⁻³⁰ DLVO theory describes total interaction energy between two particles in solution as a net result of attractive van-der Waals (vdW) forces and repulsive electrostatic double-layer (EDL) interactions (**Figure 4**). This Interaction potential barrier, which defines the colloidal stability conventionally, depends on the dimensions, dielectric and surface charges at the particle-solution interface. For, $V_{tot} < 0$, van-der waals attractive term is greater than the repulsive EDL leading to colloidal instability and aggregation of the particles. Our experiments show significant decrease in V_{tot} under optical illumination leading to enhanced rate of aggregation.

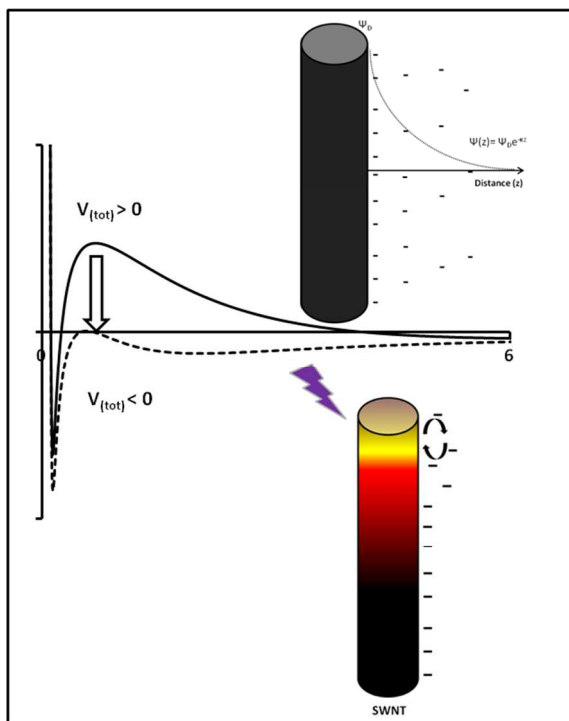


Figure 4. Conceptual model of optically induced aggregation of SWNTs from solution. The figure shows interaction potential between cylinders according to DLVO theory. Uniform surface charges are shown to be affected by the illumination in an absorbing SWNT; leading to colloidal instability.

Total potential (V_{tot}) for two interacting cylinders in solution is approximated by the following expression.¹⁶ $V_{tot} = \left(\frac{-A_H}{12\sqrt{2}D^{3/2}} + \frac{k^{1/2}}{\sqrt{2\pi}} Z e^{-kD} \right) \left[\sqrt{\frac{R_1 R_2}{R_1 + R_2}} \right]$ Where, D is surface distance between two nanotubes with radius R_1 and R_2 . A_H is the Hamaker constant in the attractive Van der Waals contribution and Z is the interaction constant of the repulsive EDL term, k^{-1} being the Debye length. According to the DLVO theory, surface charges are considered uniform and at either constant surface potential or constant charge density. Both the photo-thermal and photophoretic forces, depends on the absorption of the particles. Local kinetics and non-uniformity of surface charges in the absorbing SWNTs may affect the interaction potential leading to colloidal instability and aggregation. Thermal gradient on the surface of an absorbing

particle in resonant optical frequency is given as $\nabla\hat{T} = \frac{1}{k_p}\hat{Q}_p$, where k_p is internal heat conductivity of the particle and \hat{Q}_p is volumetric thermal energy which relates to refractive index absorbed by the wavelength of incident radiation.²⁷ It is expected that, absorption and plasmonics resonance may lead to local temperature variations depending on the thermal conductivity of the absorbing SWNTs. Since, absorption by the SWNTs depends on the diameter of the SWNTs, absorbing SWNTs of selective diameters are expected to have enhanced photo-thermal and photophoretic effects. Clearly, much research is needed, both theoretically and experimentally to better understand the phenomenon.

However, in conclusion we report the phenomenon of optically induced aggregation in selective SWNTs from pristine well dispersed solution, thereby causing separation of specific SWNTs. Rapid aggregation was observed for pure SWNT solution exposed to optical illumination by simple light sources. Results show that the rate of aggregation primarily depends on the intensity of light with selective aggregation in specific SWNTs due to frequency of illumination. Our results show that controlled optical excitation may be used for large scale efficient separation of particular diameters of SWNTs. Absorption and Raman spectra of the separated supernatant and aggregated floc especially in the NIR illumination show relative enrichment in specific SWNTs. Additional theoretical and experimental research should provide deeper fundamental understanding of the phenomenon and initiate development of efficient optical processes for separation of not just specific diameter SWNTs, but possibly of other nanoparticles from the solution too.

ACKNOWLEDGMENTS

Authors are deeply indebted to Ramanujan fellowship (SR/S2/RJN-28/2009) and funding agencies DST (DST/TSG/PT/2012/66), Nanomission (SR/NM/NS-15/2012) for generous grants.

REFERENCES

- (1). Avouris, P.; Freitag, M.; Perebeinos, V. Carbon-nanotube photonics and optoelectronics, *Nature photonics* **2008**, 2, (6), 341-350.
- (2). Bekyarova, E.; Ni, Y.; Malarkey, E. B.; Montana, V.; McWilliams, J. L.; Haddon, R. C.; Parpura, V. Applications of carbon nanotubes in biotechnology and biomedicine, *Journal of biomedical nanotechnology* **2005**, 1, (1), 3.
- (3). Hu, W.; Lu, Z.; Liu, Y.; Li, C. M. In situ surface plasmon resonance investigation of the assembly process of multiwalled carbon nanotubes on an alkanethiol self-assembled monolayer for efficient protein immobilization and detection, *Langmuir* **2010**, 26, (11), 8386-8391.
- (4). Israelachvili, J. N., *Intermolecular and surface forces: revised third edition*. Academic press: 2011.
- (5). Mitchell, C. A.; Bahr, J. L.; Arepalli, S.; Tour, J. M.; Krishnamoorti, R. Dispersion of functionalized carbon nanotubes in polystyrene, *Macromolecules* **2002**, 35, (23), 8825-8830.
- (6). Huang, S.; Fu, Q.; An, L.; Liu, J. Growth of aligned SWNT arrays from water-soluble molecular clusters for nanotube device fabrication, *Phys. Chem. Chem. Phys.* **2004**, 6, (6), 1077-1079.
- (7). Li, J.; Lu, Y.; Ye, Q.; Cinke, M.; Han, J.; Meyyappan, M. Carbon nanotube sensors for gas and organic vapor detection, *Nano Letters* **2003**, 3, (7), 929-933.
- (8). Chen, Z.; Du, X.; Du, M.-H.; Rancken, C. D.; Cheng, H.-P.; Rinzler, A. G. Bulk Separative Enrichment in Metallic or Semiconducting Single-Walled Carbon Nanotubes, *Nano Letters* **2003**, 3, (9), 1245-1249.

- (9). Maeda, Y.; Kimura, S.-i.; Kanda, M.; Hirashima, Y.; Hasegawa, T.; Wakahara, T.; Lian, Y.; Nakahodo, T.; Tsuchiya, T.; Akasaka, T. Large-scale separation of metallic and semiconducting single-walled carbon nanotubes, *Journal of the American Chemical Society* **2005**, 127, (29), 10287-10290.
- (10). Zheng, M.; Jagota, A.; Semke, E. D.; Diner, B. A.; McLean, R. S.; Lustig, S. R.; Richardson, R. E.; Tassi, N. G. DNA-assisted dispersion and separation of carbon nanotubes, *Nature materials* **2003**, 2, (5), 338-342.
- (11). Ménard-Moyon, C.; Izard, N.; Doris, E.; Mioskowski, C. Separation of semiconducting from metallic carbon nanotubes by selective functionalization with azomethine ylides, *Journal of the American Chemical Society* **2006**, 128, (20), 6552-6553.
- (12). Liu, H.; Nishide, D.; Tanaka, T.; Kataura, H. Large-scale single-chirality separation of single-wall carbon nanotubes by simple gel chromatography, *Nature communications* **2011**, 2, 309.
- (13). Arnold, M. S.; Green, A. A.; Hulvat, J. F.; Stupp, S. I.; Hersam, M. C. Sorting carbon nanotubes by electronic structure using density differentiation, *Nature nanotechnology* **2006**, 1, (1), 60-65.
- (14). Smith, D.; Woods, C.; Seddon, A.; Hoerber, H. Photophoretic separation of single-walled carbon nanotubes: a novel approach to selective chiral sorting, *Physical Chemistry Chemical Physics* **2014**, 16, (11), 5221-5228.
- (15). Madhusudana, G.; Bakaraju, V.; Chaturvedi, H. Photophoresis in Single Walled Carbon Nanotubes, *arXiv preprint arXiv:1503.07353* **2015**.
- (16). Eckstein, H.; Kreibig, U. Light induced aggregation of metal clusters, *Zeitschrift für Physik D Atoms, Molecules and Clusters* **1993**, 26, (1), 239-241.

- (17). Drachev, V. P.; Perminov, S. V.; Rautian, S. G. Optics of metal nanoparticle aggregates with light induced motion, *Optics express* **2007**, 15, (14), 8639-8648.
- (18). Satoh, N.; Hasegawa, H.; Tsujii, K.; Kimura, K. Photoinduced coagulation of Au nanocolloids, *The Journal of Physical Chemistry* **1994**, 98, (8), 2143-2147.
- (19). Chaturvedi, H.; Poler, J. Photon enhanced aggregation of single walled carbon nanotube dispersions, *Applied physics letters* **2007**, 90, (22), 223109.
- (20). Sharma, A.; Prasad, E. S.; Chaturvedi, H. Optically Induced Aggregation In Single Walled Carbon Nanotubes Functionalized with Bacteriorhodopsin, *arXiv preprint arXiv:1503.05719* **2015**.
- (21). Bachilo, S. M.; Strano, M. S.; Kittrell, C.; Hauge, R. H.; Smalley, R. E.; Weisman, R. B. Structure-assigned optical spectra of single-walled carbon nanotubes, *Science* **2002**, 298, (5602), 2361-2366.
- (22). Wilder, J. W.; Venema, L. C.; Rinzler, A. G.; Smalley, R. E.; Dekker, C. Electronic structure of atomically resolved carbon nanotubes, *Nature* **1998**, 391, (6662), 59-62.
- (23). Dresselhaus, M. S.; Dresselhaus, G.; Saito, R.; Jorio, A. Raman spectroscopy of carbon nanotubes, *Physics Reports* **2005**, 409, (2), 47-99.
- (24). Dresselhaus, M.; Saito, R.; Jorio, A. Semiconducting carbon nanotubes, *Physics of Semiconductors; Part A* **2005**, 772, 25-31.
- (25). Brown, S. D. M.; Jorio, A.; Corio, P.; Dresselhaus, M. S.; Dresselhaus, G.; Saito, R.; Kneipp, K. Origin of the Breit-Wigner-Fano lineshape of the tangential G -band feature of metallic carbon nanotubes, *Physical Review B* **2001**, 63, (15), 155414.
- (26). Murakami, T.; Nakatsuji, H.; Inada, M.; Matoba, Y.; Umeyama, T.; Tsujimoto, M.; Isoda, S.; Hashida, M.; Imahori, H. Photodynamic and photothermal effects of semiconducting

and metallic-enriched single-walled carbon nanotubes, *Journal of the American Chemical Society* **2012**, 134, (43), 17862-17865.

(27). Keh, H. J.; Tu, H. J. Thermophoresis and photophoresis of cylindrical particles, *Colloids and Surfaces A: Physicochemical and Engineering Aspects* **2001**, 176, (2), 213-223.

(28). Verwey, E.; Overbeek, J., *Theory of the stability of lyophobic colloids*. Elsevier Pub. Co., New York: 1948.

(29). Derjaguin, B.; Landau, L. Theory of the stability of strongly charged lyophobic sols and of the adhesion of strongly charged particles in solutions of electrolytes, *Progress in Surface Science* **1993**, 43, (1), 30-59.

(30). Sonntag, H.; Strenge, K.; Vincent, B.; Vincent, B., *Coagulation kinetics and structure formation*. Springer US: 1987.